ELSEVIER

Biophysical Chemistry 63 (1996) 67–80

Biophysical Chemistry

Optical activity of a nucleotide-sensitive tryptophan in myosin subfragment 1 during ATP hydrolysis

Sungjo Park, Katalin Ajtai, Thomas P. Burghardt *

Department of Biochemistry and Molecular Biology, Mayo Foundation, Rochester, MN 55905, USA

Received 3 June 1996; accepted 16 July 1996

Abstract

The xanthene probes 5′-iodoacetamido-fluorescein and -tetramethylrhodamine specifically modify skeletal muscle myosin subfragment 1 (S1) at the reactive thiol residue (SH1) and fully quench the fluorescence emission from tryptophan residue 510 (Trp510) in S1 (T.P. Burghardt and K. Ajtai, Biophys. Chem., 60 (1996) 119; K. Ajtai and T.P. Burghardt, Biochemistry, 34 (1995) 15943). The difference between the fluorescence intensity obtained from S1 and probe-modified S1 comes solely from Trp510 in chymotryptic S1, a protein fragment that contains five tryptophan residues. The rotary strength and quantum efficiency of Trp510 were measured using difference signals from fluorescence detected circular dichroism (FDCD) and fluorescence emission spectroscopy. These structure-sensitive signals indicate that the binding of nucleotide or nucleotide analogs to the active site of S1 causes structural changes in S1 at Trp510 and that a one-to-one correspondence exists between Trp510 conformation and transient states of myosin during contraction. The Trp510 rotary strength and quantum efficiency were interpreted structurally in terms of the indole side-chain conformation using model structures and established computational methods.

Keywords: Fluorescence detected circular dichroism; Nucleotide analogs; Muscle contraction; Origin independent matrix method; Myosin tryptophan 510; Probe binding cleft; ATP hydrolysis

1. Introduction

The molecular mechanism of muscle contraction involves the cyclical interaction of the myosin cross-bridge with the actin filament during hydrolysis of ATP by myosin. This mechanism separates into the two aspects of force generation and energy transduction. Force generation refers to the global structural changes in actomyosin that cause the relative translation of myosin and actin filaments in a muscle fiber during contraction. Energy transduction refers to local structural changes within the myosin head or subfragment 1 (S1) that communicate events

Abbreviations: ATP Adenosine triphosphate; (FD)CD (Fluorescence detected) circular dichroism; Cys707 or SH1 Highly reactive thiol in skeletal myosin subfragment 1; DTT Dithiothreitol; EDTA Ethylenediaminetetraacetic acid; FRET Fluorescence resonance energy transfer; IAA Iodoacetamide; PMSF Phenylmethanesulfonyl floride; PMT Photomultiplier tube; S1 Myosin subfragment 1; TME L-Tryptophan methyl ester; Trp510 Tryptophan 510 in skeletal muscle; UV Ultraviolet; 5′IAF 5′-Iodoacetamidofluorescein; 5′IATR 5′-Iodoacetamidotetramethylrhodamine; 5′F-S1 5′IAF-labeled S1; 5′R-S1 5′IATR-labeled S1

* Corresponding author. Email: burghard@mayo.edu

PII S0301-4622(96)02203-X

at the ATP binding site to the sites of force generation and actin binding. The energy transduction mechanism may involve pathways along which local conformation changes propagate through the peptide backbone from the ATP binding site to the sites of force generation and actin binding [1–3]. The path connecting the ATP binding with the force generation site must store some of the energy from ATP hydrolysis for use in work production. Two or more pathways are at work if sites of force generation and actin binding are spatially separated.

Changes in the fluorescence intensity from tryptophan residues in the cross-bridge signal the binding and hydrolysis of ATP [4] suggesting that the ATP-sensitive tryptophans in S1 are within the energy transduction pathway. The site-specific modification of S1 with spin or fluorescent probes [5,6], cross-linkers [7], activatable cross-linkers [8], or other reagents also signaled local S1 sensitivity to ATP binding and/or hydrolysis. More sophisticated techniques including fluorescence resonance energy transfer (FRET) [1–3], and imaging methods combined with rapid freezing of reactants that preserved structural integrity [9], identified and correlated structural changes in S1 with certain steps in the ATP hydrolysis cycle. The circular dichroism (CD) in the far-ultraviolet (far-UV) spectral region where the peptide backbone absorbs, showed a small but significant change due to ATP binding [10,11]. The CD in the near-UV region where the aromatic residues of S1 absorb showed larger changes in tertiary structure due to ATP binding [10,12]. The far- or near-UV CD signals from S1 do not provide a physical model for structural changes in S1 correlated with the ATPase cycle because they originate from all or several residues in the protein. The atomic coordinates of the S1 peptide backbone with and without nucleotide now form a basis for all discussion of domain movement within S1 [13–16].

The xanthene dyes 5′-iodoacetamidofluorescein (5′IAF) or 5′-iodoacetamidotetramethylrhodamine (5′IATR) specifically bind to the highly reactive thiol (SH1) in skeletal muscle S1 to make 5′R-S1 or 5′F-S1 [17,18]. Several lines of evidence from our investigation of the conformation of these probes in the SH1 binding pocket indicate that the probes interact exclusively with Trp510 [19,20]. We showed there that the probe absorption and CD spectra indicate a tight interaction (within 3–4 Å) with a tryptophan residue. Identical measurements carried out with 5′R-S1 and 5′F-S1 in the presence of nucleotide indicate a similarly tight interaction between the probe and tryptophan residue [20]. Trp510 is the only candidate for this type of complex with the probe. The surmised probe–tryptophan conformation implies that the distance from the probe to another tryptophan in S1 is beyond the characteristic distance of 25 Å for Förster energy transfer between tryptophan and rhodamine or fluorescein [19]. Consequently, the difference in the tryptophan emission intensity between S1 and 5′F-S1 or 5′R-S1 originates solely from native Trp510. We used the difference tryptophan emission signal to isolate Trp510 emission and observe the acrylamide quenching of Trp510, in the presence and absence of nucleotide or nucleotide analogs, to show that the probe binding cleft containing Trp510 and SH1 closes during ATP hydrolysis [21]. We further develop our investigation of the structure of the probe binding cleft by observing and interpreting the CD signal isolated from Trp510.

In xanthene probe modified S1 we isolate the CD signal from Trp510 by using fluorescence detected CD (FDCD) [22,23]. In FDCD chiral fluorescent chromophores like tryptophan preferentially absorb right- (+) or left- (−) handed circularly polarized light, i.e. their extinction coefficients for right- (ϵ_+) or left- (ϵ_-) handed circularly polarized light are not equal. The intensity of emitted fluorescence follows this preference since, under well-defined circumstances, the fluorophore emission intensity is proportional to $\epsilon_\pm$. If we make the difference FDCD spectrum between S1 and xanthene-modified S1 then we observe the FDCD signal originating solely from native Trp510. The isolation of the Trp510 signal also holds in the presence of nucleotide or nucleotide analogs. The native Trp510 CD spectrum cannot be isolated with transmission light detected CD because Trp510 absorbs light whether or not it is quenched, and the fluorescein, nucleotide, or nucleotide analog contributes to the CD signal in the tryptophan absorption band.

We interpret changes in the FDCD signal intensity and shape as a function of excitation wavelength in terms of a physical model of Trp510 tertiary structure using a simple molecular model and meth-

ods developed for CD [24]. The changes in FDCD and fluorescence emission from Trp510, caused by nucleotide analog binding to S1 and interpreted in terms of structural changes in the vicinity of Trp510, correlate Trp510 structure with particular chemical intermediates in the ATPase cycle. In this way we may begin to identify cyclical structural changes in the transduction pathway that occur during energy transduction.

2. Theory

2.1. The interpretation of the observed signals

The spectropolarimeter modulator produces left- or right-handed circularly polarized excitation light for illuminating the sample. The excitation light passes through the sample and is detected in CD mode by a detector placed in its path. The fluorescence emitted by the sample is detected in FDCD mode by a detector placed at 90° to the excitation beam path. We selectively detect tryptophan fluorescence using an emission filter in FDCD mode. The detector in both modes of operation is a photomultiplier tube (PMT). The spectropolarimeter detects CD by actively adjusting the PMT voltage to hold the anode DC voltage constant for all excitation wavelengths making the anode AC voltage proportional to the CD signal. The calibrated recorded signal $S_{CD} = (I_R - I_L)/(I_R + I_L)$, where $I_{R(L)}$ is the transmitted intensity for right (left) circularly polarized light, is related to the CD extinction coefficient by $\Delta\epsilon \equiv \epsilon_- - \epsilon_+ = (1/33)(90/\pi)(1/Cl)S_{CD}$, where C is the sample concentration and l is the light path length [22]. We compute the rotary strength, $R = 0.248 \int \Delta\epsilon \, d\lambda/(\lambda\beta)$ in Debye–Bohr magnetons, where β is the Lorentz correction for the polarizability of the solvent and λ the excitation light wavelength [25].

For FDCD experiments we prepare samples with total absorption at 280 nm, $A_{280} \leq 0.05$, so that the inner filtering of the excitation light and the self-absorption of emitted light are negligible. We assume for now that we can neglect energy transfer from tyrosine to tryptophan in S1. In the FDCD mode we hold the PMT voltage fixed to record the signal, $S_{FDCD} = K(F_R - F_L)$, where $F_{R(L)}$ is the fluorescence emitted after excitation by right (left) circularly polarized light and K is a constant dependent on the light collection efficiency of the spectropolarimeter. $S_{FDCD} = -KCl\sum_i \phi_i \Delta\epsilon_i$, where the sum is over the tryptophans in S1, ϕ_i is the quantum efficiency and $\Delta\epsilon_i$ the CD extinction coefficient for residue i [22]. The probe at SH1 quenches Trp510 but leaves alone the emission from all of the other residues so that the difference in the tryptophan emission in the FDCD spectra between identical protein concentration samples of S1 and 5′F-S1 originates solely from Trp510 such that

$$\Delta S_{FDCD} \equiv S_{FDCD}(S1) - S_{FDCD}(5'F - S1) = -KCl\Delta\epsilon_{510}\phi_{510} \quad (1)$$

where $\Delta\epsilon_{510}\phi_{510}$ is the product of the CD extinction coefficient and quantum efficiency of Trp510 in native S1.

We also measure the fluorescence from the sample on a fluorescence spectrometer. The difference in the tryptophan emission, ΔF, between identical protein concentration samples of S1 and 5′F-S1 originates solely from Trp510 such that

$$\Delta F \equiv F(S1) - F(5'F - S1) = K'Cl\epsilon_{510}\phi_{510} \quad (2)$$

where F is the tryptophan fluorescence intensity excited by 295 nm light, K' is a constant dependent on light collection efficiency of the fluorometer, and ϵ_{510} is the extinction coefficient of native Trp510. The isolation of Trp510 emission using Eqs. (1) and (2) is independent of the efficiency of probe modification of S1. Combining Eqs. (1) and (2) we find

$$\Delta\epsilon_{510} = -\epsilon_{510}(K'/K)(\Delta S_{FDCD}/\Delta F) \quad (3)$$

We form the ratio of signals, to avoid the necessity of determining instrument-dependent unknowns, for comparing Trp510 signals in the presence and absence (+ and −) of nucleotide or nucleotide analog, P, such that

$$\frac{D_{510}(-P)}{D_{510}(+P)}\frac{R_{510}(+P)}{R_{510}(-P)} = \frac{\Delta F(-P)}{\Delta F(+P)} \times \frac{\int \Delta S_{FDCD}(+P)\,d\lambda/\lambda}{\int \Delta S_{FDCD}(-P)\,d\lambda/\lambda} \quad (4)$$

where we have formed the rotary strength R_{510} from $\Delta\epsilon_{510}$ and replaced ϵ_{510} with the dipole strength

D_{510}. Observed/calculated quantities are on the right-/left-hand side of Eq. (4).

2.2. The effect of photoselection in FDCD

S1 does not move quickly enough to dynamically depolarize light emitted by tryptophan following excitation by circularly polarized light. Consequently, FDCD from the S1 sample is characteristic to that from an ordered sample due to the effect of photoselection. We utilize previously described methods to analyze FDCD from this system [26,27]. This problem is equivalent to the analysis of CD from oriented systems [28].

Tinoco et al. [27] calculated the effect of photoselection on the FDCD signal for several experimental possibilities. For our instrument (emitted light detected at 90° from the excitation beam), an emission polarizer at the magic angle eliminates the effect of photoselection. This possibility is undesirable in our case due to the loss of light intensity at the polarizer. We choose to detect light without an emission polarizer and to handle the effect of photoselection in the model calculation of the FDCD signal. Then, S_{FDCD} gives rotary strength, R, such that

$$R \propto R_{1,1} + R_{2,2} + (4/3)R_{3,3} \tag{5}$$

with

$$\begin{aligned} R_{1,1} = (3/2)\mathrm{Im}[(\mu)_{0a} \cdot (M)_{a0} - (\mu_1)_{0a}(M_1)_{a0}] \\ + (3/4)[(E_a - E_0)/(\hbar c)] \\ \times \mathrm{Re}[(\mu_3)_{0a}(Q_{21})_{a0} - (\mu_2)_{0a}(Q_{31})_{a0}] \end{aligned} \tag{6}$$

where operators μ, M, and $Q_{i,j}$ are the single electron operators for the electric dipole moment, the magnetic dipole moment, and the quadrupole moment, respectively. Subscripts $a0$ and $0a$ indicate matrix elements for transitions involving the ground state (0) with energy E_0 and excited state (a) with energy E_a of the coupled system, and, $\hbar c = hc/2\pi$ where h is Planck's constant and c is the speed of light [28]. Im[] or Re[] means imaginary or real part of []. $R_{2,2}$ and $R_{3,3}$ are obtained by the cyclic permutation of the indices of $R_{1,1}$ and the subscripts on R refer to coordinate axes with the 3-axis parallel to the emission transition moment of indole. $R = (1/3)(R_{1,1} + R_{2,2} + R_{3,3}) = \mathrm{Im}[(\mu)_{0a} \cdot (M)_{a0}]$ for

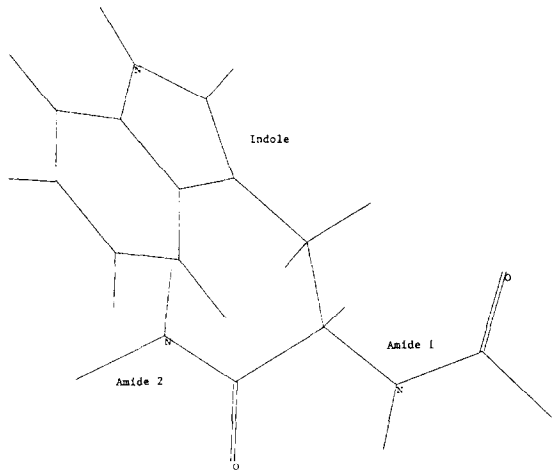

Fig. 1. The molecular model of Trp510 showing the flanking amide groups from the Glu509–Trp510–Glu511 sequence in skeletal muscle and the indole side-chain from Trp510.

dynamically depolarizing samples. The expression for $R_{i,i}$ involves magnetic and quadrupole contributions that are computed for our model of Trp510 given in Fig. 1.

2.3. The influence of structure on the optical signal

Molecular structure calculations, based on a simple model system for tryptophan in a peptide, predict conformation-sensitive optical signals for single tryptophans in S1. The agreement between calculated and observed optical signals, simple geometrical constraints, and total energy constraints guide the choice of structures for the solution set. The conformation-sensitive optical signal computation program uses the geometrical constraints to limit the degrees of freedom searched in molecular configuration space. Once conformations equivalently satisfying the optical and geometrical constraints are identified we use the total energy parameter to select among them. The optical signal constraints take priority over total energy considerations since we compute vacuum model system energies while optical signal calculations include solvent and local environment effects. We estimate total configurational energy with a molecular mechanics calculation from the commercial software package HyperChem (Hypercube Inc., Waterloo, Ontario, Canada). We address here only the methods used in the optical signal calculation.

The matrix [24] and perturbative [29,30] formulation of the optical signal were given. Both approaches produce results in good agreement with experiment despite various inherent limitations. We adopted the matrix method, modified to eliminate origin dependence in the calculated rotary strength [31], for the calculation of optical signals from the peptide. The matrix formulation couples the observable lowest energy excited states of interacting molecules by the Coulomb potential acting among the transition monopoles for these excited states to produce the total electronic wavefunction, Ψ. It is assumed that the ground state is excluded from the interaction, that configurations involving simultaneous excitation of interacting groups are neglected, and that no charge transfer occurs between interacting groups. Other assumptions implicit in this formulation are thoroughly discussed in the original literature [24,31,32]. From Ψ we compute the absorption wavelength maximum and magnitude of the dipole strength, and the magnitude and sign of the rotary strength using established methods [24,28].

Fig. 1 shows a simple model for the local structure of a peptide containing tryptophan. The model contains two trans peptide groups, amide 1 and amide 2, in a dipeptide flanking an α-carbon, and an indole group in the tryptophan side-chain. The two observable lowest energy excited states of a peptide group correspond to the (n,π^*) and the (π,π^*) transitions [24,32,33]. The four observable lowest energy excited states of indole are (π,π^*) transitions designated $(^1A_1,^1L_a)$, $(^1A_1,^1L_b)$, $(^1A_1,^1B_a)$, and $(^1A_1,^1B_b)$ [34–40]. These excited states plus the ground state form the basis set of states for our calculation. The calculation was performed for a secondary–secondary amide combination [24]. Previously, optical signals from a dipeptide, tyrosine, and a model compound containing indole were computed using the matrix methods [24,36,41]. These calculations supply the position and relative magnitude of the transition monopoles of the peptide groups and indole for use in our application.

The Ramachandran angles ϕ and ψ of the L-tryptophan residue in a peptide determine the conformation of the amides and consequently the orientation of the dipoles associated with the lowest energy amide electrically (π,π^*) and magnetically (n,π^*) allowed transitions. The torsion angles about bonds C_α–C_β and C_β–C_γ in the indole side-chain, χ_1 and χ_2 respectively, specify the relationship of indole relative to the peptide backbone. Consequently, χ_1 and χ_2 determine the orientation of the dipoles lying in the plane of the indole that are associated with the four lowest energy electric transitions $(^1A_1,^1L_a)$, $(^1A_1,^1L_b)$, $(^1A_1,^1B_a)$, and $(^1A_1,^1B_b)$. Given transition monopole charges and positions from the literature for the electric and magnetic dipoles in the amides [24], and the electric dipoles in indole [36], we compute the absorption dipole strength, peak wavelength, and rotary strength for the complex shown in Fig. 1 as a function of ϕ, ψ, χ_1, and χ_2 by the matrix formulation of the optical signal for comparison with experiment.

Fig. 1 represents the minimum model for Trp510 and we find it is sufficient to impart the observed amount of optical activity to the two lowest energy absorption bands of indole. Previous efforts to compute the near-UV CD signal from ribonuclease S, using the crystallographic coordinates of the protein atoms, showed that the signal originates from tyrosine side-chains interacting with their flanking amide groups (like our model) and with side-chains from other nearby tyrosines and histidines [42,43]. The importance of other residues on the optical signal from a given tyrosine residue depends on their relative proximity and conformation. While a more elaborate model than that in Fig. 1 for the Trp510 region of S1 is indicated on the basis of these previous findings, its structure is far too under-constrained to be helpful given only the C_α coordinates of S1. We use independent constraints, obtained from previous work on the conformation of the 5′IAF–Trp510 complex [19,20], to supplement the constraints of the model and to arrive at a suitable solution for the Trp510 structure. The model of Fig. 1 should be expanded when the crystallographic structure of the S1 side-chains becomes available to adequately constrain the more numerous degrees of freedom in a bigger model.

3. Materials and methods

3.1. Chemicals

The fluorescent labels 5′-iodoacetamidofluorescein (5′IAF) and 5′-iodoacetamidotetra-

methylrhodamine (5'IATR) were from Molecular Probes (Eugene, OR). ATPγS was from Boehringer Mannheim (Indianapolis, IN). L-Tryptophan methyl ester (TME) was from Aldrich (Milwaukee, WI). ATP, ADP, phenylmethanesulfonyl floride (PMSF), ethylenediaminetetraacetic acid (EDTA), dithiothreitol (DTT), and iodoacetamide (IAA) were from Sigma (St. Louis, MO). All chemicals were analytical grade.

3.2. Solutions

A stock solution of $BeCl_2$ (Be, atomic absorption standard solution, in 1% HCl) was adjusted to pH 5.0 by addition of NaOH. A stock solution of sodium vanadate was made by the method of Goodno [44]. A stock solution of NaF was prepared freshly each day in a plastic bottle. Our standard buffer was 25 mM TES buffer at pH 7.0, labeling buffer was standard buffer plus 0.2 mM PMSF, and protein buffer was labeling buffer plus 1 mM DTT.

3.3. Preparation and labeling of myosin subfragment 1

Rabbit myosin was prepared by a standard method [45]. We prepared S1 by digesting myosin filaments with α-chymotrypsin [46]. S1 at 10–25 μM concentration was labeled with 1.2- to 1.6-fold molar excess of 5'IATR or 5'IAF in labeling buffer for 12 h at 4°C. IAA treatment of S1 was performed in labeling buffer with a 10-fold molar excess of IAA. Under these conditions 5'IATR modified 41% [47], 5'IAF modified 60–70% [18], and IAA modified about 83% of the SH1s on S1. The stoichiometry and specificity of 5'IATR, 5'IAF, and IAA for SH1 on S1 were characterized as described previously [18,47,48]. After labeling, 1 mM DTT was added (making protein buffer) to stop further modification of the SHs by free label.

Unreacted dye did not affect tryptophan emission from S1 and was usually not removed from the samples. A sample of unmodified S1 was prepared and handled identically to the modified protein. Labeled and unlabeled S1 samples had identical protein concentrations so that their tryptophan fluorescence intensities could be directly compared. Samples for FDCD or fluorescence measurements were diluted to have < 0.05 absorbance at 280 nm.

3.4. Preparation of S1–nucleotide analog complexes

We prepared the S1–nucleotide analog complexes by the method of Werber et al. [49]. For beryllium and aluminum analogs, 0.6 μM S1 in 25 mM TES at pH 7.0 was mixed with 1 mM $MgCl_2$, 3 μM ADP, 2 mM NaF, and 0.2 mM $AlCl_3$ or 0.2 mM $BeCl_2$ for 15–20 min at 21°C. For the vanadate analog S1 was mixed with 1 mM $MgCl_2$, 15 μM vanadate, and 3 μM ADP for 15–20 min at 21°C. Analogs complexed with S1 with 80–90% efficiency as measured by S1 K^+EDTA ATPase inhibition.

3.5. Spectroscopic measurements

We measured absorption spectra on a Beckman DU650 (Beckman Instruments, Fullerton, CA) spectrophotometer with spectral resolution of 2 nm. All absorption measurements were made at 10°C.

We collected FDCD spectra on a Jasco J720 spectropolarimeter modified with an FDCD attachment (Jasco Inc., Tokyo, Japan). The FDCD attachment is a rectangular 1-cm path length temperature-controlled cell holder with an opening to permit detection of fluorescence at 90° from the excitation light path. Fluorescence is detected by the PMT of the spectropolarimeter mounted at 90° from the excitation light path. Spectra were collected at fixed photomultiplier voltage (500 V) and with 2 nm bandwidth excitation light. Emission from the indole groups in tryptophan was selected using a bandpass filter transmitting light at 400 ± 50 nm. All protein spectra were signal averaged for approximately 24 min immediately following preparation. All FDCD measurements were made at 9.5 ± 1.5°C.

We measured fluorescence on an SLM 8000 spectrofluorometer (SLM Instruments, Urbana, IL). Spectra were recorded with monochromator slits of 2–4 nm. Tryptophan emission spectra were recorded with an excitation wavelength of 295 nm. Tryptophan emission intensity ratios, used in Eq. (4), were formed at an emission wavelength of 336 nm or using the integrated area under the emission band from 320–354 nm. Tyrosine and tryptophan excitation spectra from labeled or unlabeled S1 were recorded with emission wavelengths of 303 and 370 nm, respectively. Excitation spectra from TME were recorded with an emission wavelength of 340 nm. Protein

spectra were signal averaged for several minutes immediately following preparation. All fluorescence measurements were made at 10°C.

3.6. Curve fitting

We fitted spectra for estimating dipole and rotary strengths. We used a least squares protocol with equality and inequality constraints [50] for locating the best linear parameters (amplitudes) during curve fitting. The best nonlinear parameters (spectral maxima and widths) were found by grid search. We assumed the shapes of the ($^1A_1$,^1L_a) and ($^1A_1$,^1L_b) transitions in indole or tryptophan to be those observed using fluorescence excitation polarization spectroscopy of indole or tryptophan [37]. These complicated spectral shapes were first closely fitted by a sum of Gaussian distributions and then this shape used to fit other spectra containing indole or tryptophan.

4. Results

4.1. Absorption measurements

We measured the absorption spectrum of indole in labeling buffer (without PMSF) and curve fitted the extinction coefficient spectrum to determine the dipole strength and wavelength maximum of the four observable lowest energy transitions ($^1A_1$,^1L_a), ($^1A_1$,^1L_b), ($^1A_1$,^1B_a), and ($^1A_1$,^1B_b). Table 1 summarizes the results of these measurements. The relative transition monopole charges for indole, obtained from the literature [36], are normalized such that the transition dipole strength, computed by summing the dipole moments from the transition monopoles charges distributed over the backbone atoms in indole, gives the values in Table 1. We did not measure dipole strengths for the peptide transitions but used the absolute transition monopole charges given previously [24].

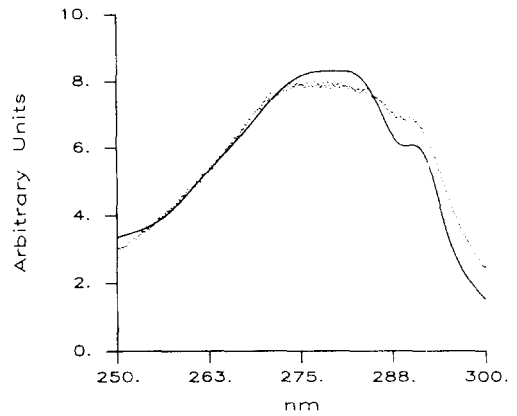

Fig. 2. The excitation spectrum of S1 in protein buffer (dots) and the fit (solid line) constructed from TME in standard buffer. Emission from S1 is collected at 370 nm.

4.2. Fluorescence measurements

4.2.1. FRET from tyrosine to tryptophan in S1

Fig. 2 shows the excitation spectrum of S1 when emission is selectively collected from tryptophan. FRET from tyrosine to tryptophan residues in S1 would influence the shape of this spectrum by contributing a component of tyrosine absorption proportional to the efficiency of energy transfer. Tyrosine to tryptophan FRET has a characteristic distance of about 14 Å [51] and all of the tryptophan C_αs in S1 have one or more of the 37 tyrosine C_αs within this characteristic distance. Inspection of the shape of the spectrum, however, suggests nearly exclusive tryptophan absorption. We quantified this observation by estimating the amount of tyrosine absorption in the

Table 1
Dipole strengths and wavelength maxima from indole in standard buffer at 10°C

	Transition			
	($^1A_1$,^1L_a)	($^1A_1$,^1L_b)	($^1A_1$,^1B_a)	($^1A_1$,^1B_b)
Dipole strength/Debye^2	5.4	0.95	18.3	16.0
Wavelength maximum/nm	267.0	275.3 [a]	215.5	196.8

[a] Average of two peaks.

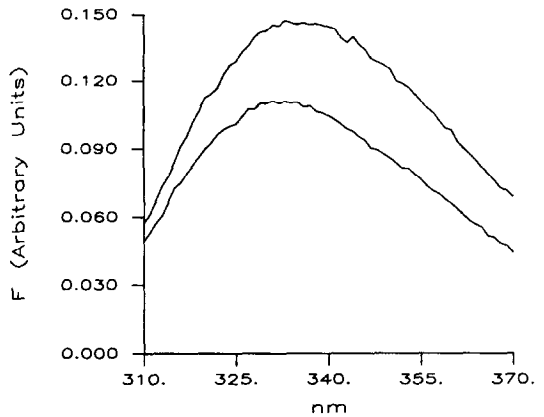

Fig. 3. Emission spectra from S1 (top) and 5'F-S1 showing the quenching of Trp510 by 5'IAF. Excitation is at 295 nm.

spectrum. We measured the tyrosine excitation spectrum of S1, and, assuming no phenylalanine to tyrosine or tryptophan to tyrosine energy transfer (or other spectral contamination), used this shape as a model for tyrosine absorption in S1. We modeled tryptophan absorption in S1 with TME in labeling buffer.

We fitted the S1 excitation spectrum with a linear combination of the tyrosine and TME excitation spectral shapes by allowing the amplitudes of these shape functions to be unknowns and permitting the TME and tyrosine spectra to shift in wavelength. The best fit indicates no contribution from tyrosine absorption. We made identical observations on similar excitation spectra obtained from 5'F-S1, 5'R-S1, and the difference between 5'F-S1 and S1. The solid line in Fig. 2 shows the best fit to the S1 excitation spectrum. We propose that the deviation of the model and S1 spectra is from structural and environmental differences between the tryptophan residues in S1 and TME.

4.2.2. S1 and modified S1

Fig. 3 shows the tryptophan emission spectra from identical concentrations of S1 and 5'F-S1. Similar spectra were measured from S1 and 5'F-S1 with bound nucleotide analogs, and S1 and 5'R-S1 in the presence and absence of bound nucleotide analogs. We formed the difference spectrum between S1 and labeled S1, ΔF, to obtain the emission spectrum of Trp510. In each condition the ratio of the ΔFs of Trp510 in the absence and presence of bound nucleotide analog was computed. Our findings are summarized in the first column of numbers in Table 2.

We studied the effect of IAA modification of SH1 on tryptophan emission. The tryptophan fluorescence emission spectra from identical concentrations of S1 and IAA-S1 had identical intensities and shape. These data indicate no observable effect on tryptophan emission due to modification of SH1 with IAA. We also compared these emission spectra in the presence of MgATP. Then spectral shape remained unchanged and the ratio of fluorescence intensities F(IAA-S1 + MgATP)/F(S1 + MgATP) = 0.94 ± 0.03 (s.e.m.,

Table 2
Quantum efficiency and rotary strength changes for Trp510 [a]

Analog	$\frac{\Delta F(-P)}{\Delta F(+P)}$ [b]	$\frac{\int \Delta S_{FDCD}(+P)d\lambda/\lambda}{\int \Delta S_{FDCD}(-P)d\lambda/\lambda}$ [c]	$\frac{\Delta F(-P)/\Delta S_{FDCD}(+P)d\lambda/\lambda}{\Delta F(+P)/\Delta S_{FDCD}(-P)d\lambda/\lambda}$ [d]	$\frac{D_{510}(-P)R_{510}(+P)}{D_{510}(+P)R_{510}(+P)}$ [e]
ADPVi	0.78 ± 0.12(6) [f]	0.86 ± 0.13(6)	0.62 ± 0.07(6)	0.56
ADPBeF$_x$	0.51 ± 0.06(4)	1.38 ± 0.17(4)	0.68 ± 0.07(4)	–
ADPAlF$_4^-$	0.62 ± 0.05(4)	1.45 ± 0.30(4)	0.88 ± 0.17(4)	–
ADP	0.76 ± 0.07(4)	1.40 ± 0.21(4)	1.03 ± 0.09(4)	–
ATPγS	0.44 ± 0.15(2)	1.10 ± 0.04(2)	0.49 ± 0.18(2)	–

[a] Rotary strengths are the sum of contributions from the indole transitions ($^1A_1$,^1L_a) and ($^1A_1$,^1L_b).
[b] $\Delta F \equiv F(S1) - F(5'F\text{- or }5'R\text{-}S1)$ and +P or −P implies with or without nucleotide analog.
[c] $\Delta S_{FDCD} \equiv S_{FDCD}(S1) - S_{FDCD}(5'F\text{-}S1 \text{ or } 5'R\text{-}S1)$.
[d] The quantity is different than multiplying column 1 and 2 in this table because the fluorescence and FDCD measurements from the same preparation were multiplied and then the products were averaged from the different preparations.
[e] Theoretical values.
[f] Errors are standard error of the mean with (n) observations.

$n = 3$) indicating a slight tendency for IAA modification of SH1 to diminish the intensity of tryptophan emission in the presence of MgATP.

4.3. FDCD measurements

Fig. 4 shows FDCD spectra from identical concentrations of S1 and 5'F-S1. The excitation wavelength covers the wavelength domain of the ($^1A_1$,^1L_a) and ($^1A_1$,^1L_b) transitions in indole. We did not attempt to collect data from higher energy indole transitions since they overlap with the peptide backbone transitions. Fig. 5 shows the difference spectrum between S1 and 5'F-S1, and the similar difference spectrum in the presence of MgADPVi. Spectra in Fig. 5 were normalized such that the relative magnitudes are corrected for Trp510 fluorescence intensity changes due to the binding of the MgADPVi. The ratio of rotary strengths computed from the spectra in Fig. 5 is the experimental value for the right-hand side of Eq. (4). The rotary strength ratios for all of the nucleotide analogs are summarized in the second column of numbers in Table 2.

We fitted FDCD difference curves, like the one in Fig. 5, to estimate the relative contributions from the indole transitions ($^1A_1$,^1L_a) and ($^1A_1$,^1L_b) to the Trp510 emission as described in Section 3.6. We obtained a range of values for the relative contributions from ($^1A_1$,^1L_a) and ($^1A_1$,^1L_b) in Trp510 suggesting that the difference spectra have too low a signal-to-noise ratio to reliably estimate this quantity.

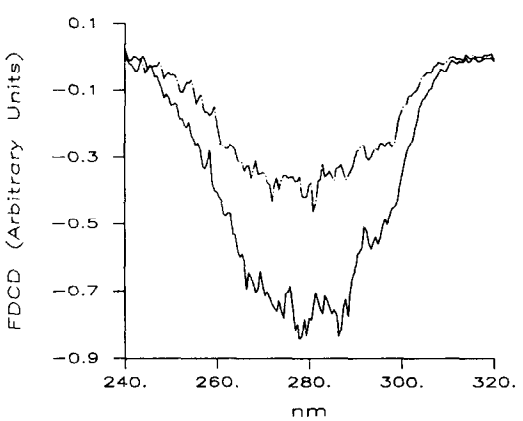

Fig. 4. FDCD excitation spectra from S1 (solid line) and 5'F-S1 (broken line). Negative FDCD corresponds to positive $\Delta\epsilon$.

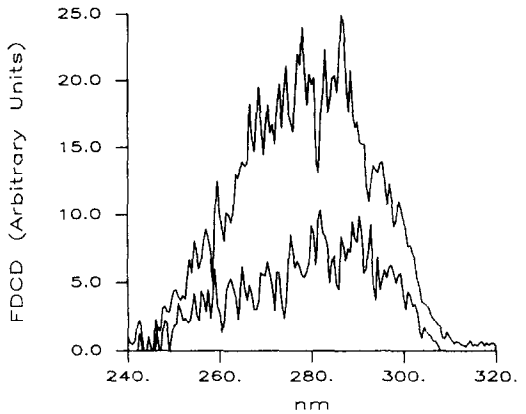

Fig. 5. Sign-reversed FDCD excitation spectra formed from the difference between S1 and 5'F-S1 in the absence (top) and presence (bottom) of MgADPVi. Spectra are normalized using quantities observed by independent fluorescence measurements such that their relative height is equal to the right-hand side of Eq. (4).

The contributions from these transitions were always in the relationship $R_{510}(^1A_1,^1L_a) > R_{510}(^1A_1,^1L_b) > 0$.

We studied the effect of IAA modification of SH1 on tryptophan FDCD. The tryptophan FDCD spectra from identical concentrations of S1 and IAA-S1 had identical intensities and shape. These data indicate that the structural aspects of the tryptophan residues in S1 indicated by FDCD are unperturbed by modification of SH1.

4.4. Structure calculation

We calculated the structure of Trp510 in the presence and absence of MgADPVi by the method outlined in Section 2. The independently adjustable parameters (ϕ, ψ, χ_1, χ_2) were varied over their angular domains with a step size of 2° thereby generating $(360/2)^4$ structures for consideration. Structures in the solution set satisfied the following criteria. (i) The distance between atoms in amides 1 and 2, and amides 1 or 2 and indole were ≥ 2.2 Å apart (excluding the distance between C and N in C–C_α–N connecting amides 1 and 2). (ii) The Trp510 Ramachandran angles (ϕ, ψ) satisfied S1 structural constraints for C_αs from Glu509, Trp510, and Glu511 [13]; they were within the domain of values

known to be allowed for the *Dictyostelium discoideum* truncated S1 main chain [14–16], and, since they determine the position of the C_β carbon in tryptophan, they satisfied the constraints contained within the requirement that 5'IAF or 5'IATR modifying SH1 interact with Trp510 with known conformation [20]. The Ramachandran angles are constrained by the C_αs from S1 in the absence of nucleotide so that our solution set will necessarily account for structural differences between S1 in the absence and presence of MgADPVi as changes in the tertiary structure of Trp510. (iii) The rotary strengths attributable to the $(^1A_1,^1L_a)$ and $(^1A_1,^1L_b)$ transitions have the relationship $R_{510}(^1A_1,^1L_a) > R_{510}(^1A_1,^1L_b) > 0$. (iv) The computed Trp510 rotary and dipole strengths, in the absence and presence of MgADPVi, satisfy Eq. (4) and the observations summarized in Table 2.

The protons on C_α and C_β of Trp510 were not used to produce the optical signal and were not accounted for in the optical signal calculation. We used molecular mechanics energy minimization (MM + force field on HYPERCHEM) to position these protons appropriately in the structure and then the whole model was reevaluated for atomic clashes using the total energy parameter. The structural differences between models satisfying criteria (i)–(iv) were in the position of indole relative to the peptide backbone. We considered the candidates energetically indistinguishable when the energy difference was half of the average energy fluctuation of indole at 10°C, i.e. 5–10 kcal mol^{-1}. We refer to this energy criteria for scoring candidate structures as criteria (v).

Candidate structures for Trp510 in the absence of nucleotide (rigor) satisfy conditions (i) through (iii) and (v). Trp510 structures in this solution set have nearly identical structures and insignificant energy differences. Fig. 6 shows a representative structure for Trp510 in rigor. Candidate structures for Trp510 in the presence of MgADPVi satisfy conditions (i) through (v). Trp510 structures in this solution set have nearly identical structures and insignificant energy differences. The energy minimization of the MgADPVi structures, while constraining the C_α positions, causes relaxation to the structure in rigor. Fig. 6 shows a representative structure for Trp510 in the presence of MgADPVi. The difference between

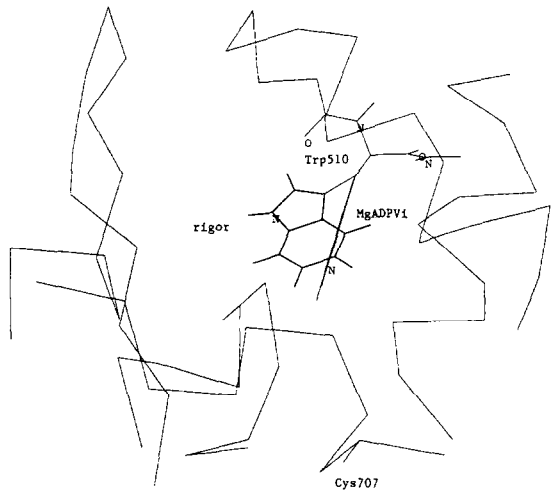

Fig. 6. The probe binding cleft of chicken S1 containing Trp510 and SH1 constructed from the crystallographic C_α coordinates [13], and the proposed effect of the binding of MgADPVi on the conformation of Trp510. The plane of the indole group in rigor (the absence of nucleotide or nucleotide analog) in bold lines is nearly parallel to the peptide backbone while in the presence of MgADPVi it is perpendicular to the plane of the projection shown.

the structure of Trp510 in the absence and presence of MgADPVi, proposed in Fig. 6, is in the position of the indole relative to the peptide backbone as expected. The energy difference between these structures, about 2 kcal mol^{-1}, is small compared to the average energy fluctuation expected for indole at 10°C.

The computed rotary and dipole strengths for the Trp510 structures in Fig. 6 in the absence and presence of MgADPVi are summarized by the ratio given in Table 2. The structures shown in Fig. 6 correspond to $(\phi,\psi) = (-169°,99°)$, and $(\chi_1,\chi_2) = (91°,-61°)$ or $(70°,-18°)$ for Trp510 in the absence or presence of MgADPVi.

5. Discussion

5.1. Tyrosine to tryptophan FRET in S1

We concern ourselves with FRET from tyrosine to tryptophan since we formulated the interpretation of FDCD signals from S1 assuming negligible FRET between these residues. The S1 fluorescence excitation spectrum in Fig. 2, collected at an emission

wavelength selective for tryptophan emission, has features similar to that of a tryptophan absorption spectrum. FRET from tyrosine to tryptophan would influence the shape of the S1 spectrum by contributing a component of tyrosine absorption proportional to the efficiency of energy transfer. We estimated the extent of tyrosine to tryptophan FRET in S1 by a method based on the similar analysis of energy transfer efficiencies among the aromatic residues in proteins [52,53]. We found that there was no significant contribution of tyrosine to the S1 excitation spectrum in Fig. 2.

5.2. *Effect of SH1 modification on tryptophans in S1*

The ATPases of S1 show that structural changes occur in the protein when SH1 is modified. It is well known that K^+-EDTA ATPase is inhibited while Ca^{2+}-activated ATPase is activated relative to control S1 with modification of SH1 [54]. SH1 modification could involve a secondary or tertiary structural change of S1 that effects the local environment of any of the tryptophan residues. In this case, if (i) the effect of modification alters the local environment of only Trp510, then the difference spectrum between S1 and modified S1 will continue to exclude emission from all of the tryptophans other that Trp510. However, if (ii) the modification alters another tryptophan, then the difference spectrum between S1 and modified S1 will not perfectly exclude the emission from other tryptophans. The latter possibility could prevent the interpretation of the difference spectrum as originating from a single tryptophan. We addressed this possibility by comparison of tryptophan fluorescence emission and FDCD signals from S1 and IAA-S1. IAA specifically modifies SH1 and alters ATPases like fluorescent probe modification of SH1 [45], but its small size prevents it from direct interaction with Trp510. We found that IAA modification of S1 did not significantly perturb its tryptophan emission or FDCD signals. We concluded that the modification SH1 does not significantly alter secondary or tertiary structure that affects the local environment of any of the tryptophan residues.

5.3. *The effect of nucleotide on Trp510 structure*

One well-studied aspect of the response of S1 to ATP binding is the increase in its tryptophan emission intensity [4,55]. Some suggest that the ATP-sensitive tryptophan is Trp510 [11,56–58], but other candidates, Trp131 and/or Trp113 [59,60], are known to be close to the ATP binding site [13]. The ATP-sensitive tryptophan showed that the stable complexes of ADP with vanadate, beryllofluoride, or aluminofluoride bound to S1 mimic the ATPase intermediates [49]. It is widely accepted that these nucleotide analogs are important tools in the investigation of the structural changes in S1 accompanying energy transduction [14–16].

We observed the effect of nucleotide or nu-

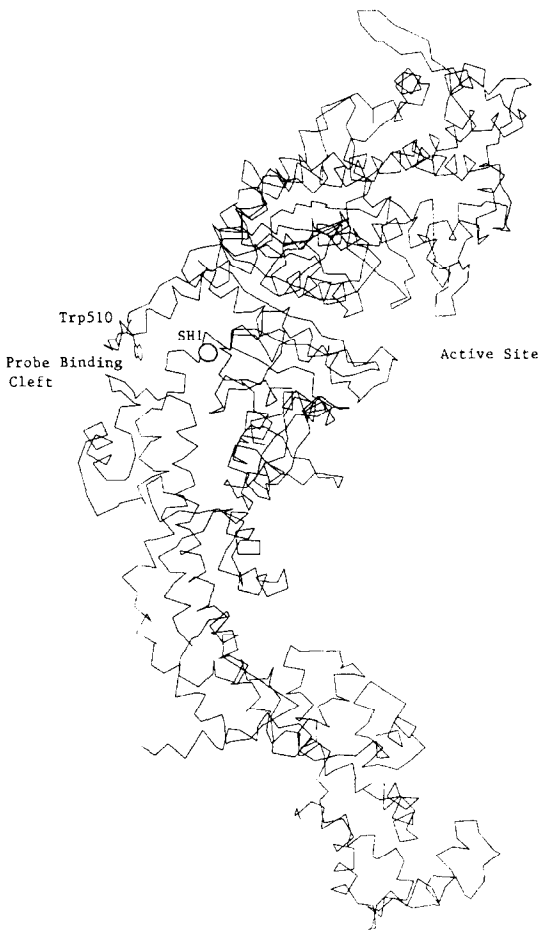

Fig. 7. The probe binding cleft of chicken S1 containing Trp510 and SH1 constructed from the crystallographic C_α coordinates [13]. From this view it appears that the upper border of the probe binding cleft and the lower border of the active site are common.

cleotide analogs on the conformation of the probe binding cleft, shown in Fig. 7, using the acrylamide quenching of Trp510 emission [21]. In these experiments we isolated Trp510 emission by forming the difference fluorescence intensity, ΔF (see Eq. (2)), and measured ΔF as a function of acrylamide concentration. The observed quenching constant is linear confirming that a single species, Trp510, is quenched. The quenching constant, characteristic to the accessibility of Trp510 to solvent, depended on the kind of nucleotide or nucleotide analog occupying the active site of S1. The solvent accessibility of Trp510 correlated with the type of nucleotide analog occupying the active site in a manner indicating that the probe binding cleft closes during ATP hydrolysis.

We observed the changes in FDCD from Trp510, caused by the trapping of MgADP by vanadate in the active site of S1, and interpreted these spectroscopic changes in terms of structural changes in the vicinity of Trp510 using model calculations and other constraints on Trp510 structure. Fig. 6 shows a comparison of the proposed Trp510 structure, within the C_α structure of S1 [13], in the absence and presence of vanadate-trapped MgADP. In the absence of nucleotide analog, Trp510 has the long axis of its indole side-chain roughly parallel to the extended peptide backbone. In the presence of MgADPVi, the long axis of the indole group has rotated to become nearly perpendicular to the peptide backbone.

Fig. 8 shows Trp510 structure in the presence of MgADPVi and while interacting with 5'IAF modifying SH1 without nucleotide. Previously, we identified the likely 5'IAF–indole conformation in S1 [19,20]. The model shown in Fig. 8 is identical to that presented there but now fitted to the C_β position surmised from our estimates of the Ramachandran angles for Trp510. We made a similar fit of the 5'IATR dimer to Trp510 (model not shown). The Ramachandran angles for Trp510 are: (i) consistent with the C_α structure of S1, (ii) within the domain of values known to be allowed for the *Dictyostelium discoideum* truncated S1 main-chain [14–16], and (iii) fit appropriately to the 5'IAF–indole complex. The Trp510 indole side-chain has similar conformations in the presence of nucleotide analog and when interacting with 5'IAF or 5'IATR. The similar proteolytic enzyme cutting pattern for S1 with nucleotide, or 5'R-S1 without nucleotide [18], suggests that these proteins share Trp510 and potentially other sites of structural correspondence.

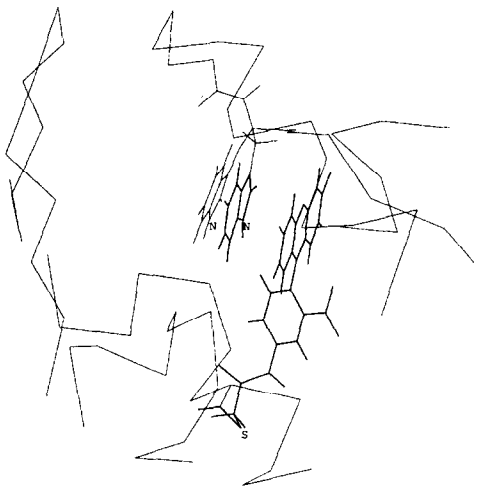

Fig. 8. The probe binding cleft of chicken S1 containing Trp510, SH1, and 5'IAF, constructed from the crystallographic C_α coordinates [13] for comparison of Trp510 structure in the presence of MgADPVi and when interacting with 5'IAF bound to SH1. The indole conformation in the presence of 5'IAF in bold lines is closest to the probe.

5.4. Implications for the molecular mechanism of muscle contraction

The structures of Trp510 presented in Figs. 6 and 8 were chosen for the solution set because they satisfied the five criteria listed in Section 4.4. Important among these criteria is how we restricted the choices for the Ramachandran angles. Future work on S1 crystallography will eventually produce the atomic coordinates of all the atoms in the peptide backbone and consequently the Ramachandran angles. Until then we rely on the observation that the chosen Ramachandran angles satisfy the constraints imposed by the C_αs and the previously determined conformation of the Trp510–5'IAF complex.

S1 undergoes global structural changes upon nucleotide or nucleotide analog binding that are presumed to be important in force generation [61–64]. The opening and closing of the probe binding cleft, due to nucleotide binding at the active site of S1, is a possible mechanism for the global structural change in S1 [15,21]. Fig. 7 shows the relationship of the probe binding cleft to the neck segment of S1. One

possibility for the coupling of cleft conformation and force production has the neck region of S1 swinging while the domain containing the active site and Trp510 remains static [13]. Our data indicate that significant structural changes are also occurring at Trp510. In our model calculations we accounted for changes observed in the FDCD signal from Trp510 as tertiary structural change in Trp510; however, at present we cannot determine whether or not these signal changes are also consistent with more global structural changes in the domain of S1 containing Trp510.

Table 2 summarizes the effect of the other nucleotide analogs on fluorescence and FDCD spectroscopy from Trp510. There it is shown that the structure-sensitive optical signal from Trp510 is perturbed by the binding of nucleotide analogs to S1 (see the third column of numbers in Table 2). The perturbation is largest for MgADPVi, smallest for MgADP, and the other analogs fall in between (the MgATPγS result is too uncertain to rank). These nucleotide analogs mimic different chemical intermediates in the ATPase cycle suggesting that there is a one-to-one correlation between transition states of myosin and the conformation of Trp510.

Acknowledgements

This work was supported by the National Institutes of Health grant R01AR39288, the American Heart Association Grant-in-Aid 930-06610, and the Mayo Foundation.

References

[1] J. Botts, R. Takashi, P.M. Torgerson, T. Hozumi, A. Muhlrad, D. Mornet and M.F. Morales, Proc. Natl. Acad. Sci. USA, 81 (1984) 2060.
[2] C.G. dos Remedios, M. Miki and J.A. Barden, J. Muscle Res. Cell Motility, 8 (1987) 97.
[3] J. Botts, J.F. Thomason and M.F. Morales, Proc. Natl. Acad. Sci. USA, 86 (1989) 2204.
[4] M.M. Werber, A.G. Szent-Gyorgyi and G.D. Fasman, Biochemistry, 11 (1972) 2872.
[5] J. Quinlivan, H.M. McConnell, L. Stowring, R. Cooke and M.F. Morales, Biochemistry, 8 (1969) 3644.
[6] J. Duke, R. Takashi and M.F. Morales, Proc. Natl. Acad. Sci. USA, 73 (1976) 302.
[7] J.A. Wells and R.G. Yount, Methods Enzymol., 85 (1982) 93.
[8] L. Szilágyi, M. Bálint, F. Sréter and J. Gergely, Biochem. Biophys. Res. Commun., 87 (1979) 936.
[9] K. Hirose, T.D. Lenart, J.M. Murray, C. Franzini-Armstrong and Y.E. Goldman, Biophys. J., 65 (1993) 387.
[10] W.D. McCubbin and C.M. Kay, Methods Enzymol., 85 (1982) 677.
[11] W.C. Johnson, Jr., D. Bivin, K. Ue and M.F. Morales, Proc. Natl. Acad. Sci. USA, 88 (1991) 9748.
[12] A.J. Murphy, Arch. Biochem. Biophys., 163 (1974) 290.
[13] I. Rayment, W.R. Rypniewski, K. Schmidt-Bäse, R. Smith, D.R. Tomchick, M.M. Benning, D.A. Winkelman, G. Wesenberg and H.M. Holden, Science, 261 (1993) 50.
[14] A.J. Fisher, C.A. Smith, J.B. Thoden, R. Smith, K. Sutoh, H.M. Holden and I. Rayment, Biophys J., 68 (1995) 19s.
[15] A.J. Fisher, C.A. Smith, J.B. Thoden, R. Smith, K. Sutoh, H.M. Holden and I. Rayment, Biochemistry, 34 (1995) 8960.
[16] C.A. Smith and I. Rayment, Biochemistry, 34 (1995) 8973.
[17] R. Takashi, Biochemistry, 18 (1979) 5164.
[18] K. Ajtai and T.P. Burghardt, Biochemistry, 31 (1992) 4275.
[19] T.P. Burghardt and K. Ajtai, Biophys. Chem., 60 (1996) 119.
[20] K. Ajtai and T.P. Burghardt, Biochemistry, 34 (1995) 15943.
[21] S. Park, K. Ajtai and T.P. Burghardt, Biochim. Biophys. Acta, 1296 (1996) 1.
[22] I. Tinoco and D. Turner, J. Am. Chem. Soc., 98 (1976) 6453.
[23] D. Turner, Methods Enzymol., 49 (1978) 199.
[24] P.M. Bayley, E.B. Nielsen and J.A. Schellman, J. Phys. Chem., 73 (1969) 228.
[25] J.A. Schellman, Chem. Rev., 75 (1975) 323.
[26] I.Z. Steinberg and B. Ehrenberg, J. Chem. Phys., 61 (1974) 3382.
[27] I. Tinoco, Jr., B. Ehrenberg and I.Z. Steinberg, J. Chem. Phys., 66 (1977) 916.
[28] J. Snir and J.A. Schellman, J. Phys. Chem., 77 (1973) 1653.
[29] I. Tinoco, Jr., J. Chem. Phys., 33 (1960) 1332.
[30] I. Tinoco, Jr., J. Chem. Phys., 34 (1961) 1067.
[31] V. Rizzo and J.A. Schellman, Biopolymers, 23 (1984) 435.
[32] J.A. Schellman and E.B. Nielsen, J. Phys. Chem., 71 (1967) 3914.
[33] E.B. Nielsen and J.A. Schellman, J. Phys. Chem., 71 (1967) 2297.
[34] Y. Yamamoto and J. Tanaka, Bull. Chem. Soc. Jpn., 45 (1972) 1362.
[35] C.-T. Chang, C.-Y. Wu, A.R. Muirhead and J.R. Lombardi, Photochem. Photobiol., 19 (1974) 347.
[36] W.J. Goux, T.R. Kadesch and T.M. Hooker, Jr., Biopolymers, 15 (1976) 977.
[37] B. Valeur and G. Weber, Photochem. Photobiol., 25 (1977) 441.
[38] L.A. Phillips and D.H. Levy, J. Chem. Phys., 85 (1986) 1327.
[39] B. Albinsson, M. Kubista, B. Nordén and E.W. Thulstrup, J. Phys. Chem., 93 (1989) 6646.
[40] P. Ilich and F.G. Prendergast, Biopolymers, 32 (1992) 667.
[41] T.M. Hooker, Jr., and J.A. Schellman, Biopolymers, 9 (1970) 1319.

[42] E.H. Strickland, Biochemistry, 11 (1972) 3465.
[43] W.J. Goux and T.M. Hooker, Jr., J. Am. Chem. Soc., 102 (1980) 7080.
[44] C. Goodno, Methods Enzymol., 85 (1982) 116.
[45] Y. Tonomura, P. Appel and M.F. Morales, Biochemistry, 5 (1966) 515.
[46] A. Weeds and R.S. Taylor, Nature (London), 257 (1975) 54.
[47] K. Ajtai, P.J.K. Ilich, A. Ringler, S. Sedarous, D.J. Toft and T.P. Burghardt, Biochemistry, 31 (1992) 12431.
[48] K. Ajtai and T.P. Burghardt, Biochemistry, 28 (1989) 2204.
[49] M.M. Werber, Y.M. Peyser and A. Muhlrad, Biochemistry, 31 (1992) 7190.
[50] G. Strang, Introduction to Applied Mathematics, Wellesley, MA, 1986, pp. 87–137.
[51] J.R. Lakowicz, Principles of Fluorescence Spectroscopy, Plenum Press, New York, 1983, pp. 348.
[52] J. Eisinger, Biochemistry, 8 (1969) 3902.
[53] Y. Saito, H. Tachibana, H. Hayashi and A. Wada, Photochem. Photobiol., 33 (1981) 289.
[54] E. Reisler, Methods Enzymol., 85 (1982) 84.
[55] M.M. Werber, Y.M. Peyser and A. Muhlrad, Biochemistry, 26 (1987) 2903.
[56] T. Hiratsuka, J. Biol. Chem., 267 (1992) 14949.
[57] D.B. Bivin, S. Kubota, R. Pearlstein and M.F. Morales, Proc. Natl. Acad. Sci. USA, 90 (1993) 6791.
[58] S.J. Papp and S. Highsmith, Biochim. Biophys. Acta, 1202 (1993) 169.
[59] Y. Okamoto and R.G. Yount, Proc. Natl. Acad. Sci. USA, 82 (1985) 1575.
[60] Y.M. Peyser, A. Muhlrad and M.M. Werber, FEBS Lett., 259 (1990) 346.
[61] S. Highsmith and D. Eden, Biochemistry, 25 (1986) 2237.
[62] S. Highsmith and D. Eden, Biochemistry, 29 (1990) 4087.
[63] K. Wakabayashi, M. Tokunaga, I. Kohno, Y. Sugimoto, T. Hamanaka, Y. Takezawa, T. Wakabayashi and Y. Amemiya, Science, 258 (1992) 443.
[64] M. Whittaker, E. Wilson-Kubalek, J.E. Smith, L. Faust, R.A. Milligan and H.L. Sweeney, Nature (London), 378 (1995) 748.